3862 *Biochemistry* **2010,** *49,* 3862–3867
DOI: 10.1021/bi100354a

BIOCHEMISTRY
including biophysical chemistry & molecular biology
Article

Determinants for Phosphodiesterase 6 Inhibition by Its γ-Subunit†

Zhongming Zhang and Nikolai O. Artemyev*

Department of Molecular Physiology and Biophysics, University of Iowa Carver College of Medicine, Iowa City, Iowa 52242

Received March 8, 2010; Revised Manuscript Received April 7, 2010

ABSTRACT: The interaction of phosphodiesterase 6 (PDE6) with its inhibitory Pγ-subunits (Pγ) is unparalleled among PDE families and is central to vertebrate phototransduction. The C-terminus of Pγ occludes the active site of PDE6, thereby preventing hydrolysis of cGMP. In this study, we examine the determinants of this critical interaction using structure-based loss-of-function mutagenesis of a chimeric PDE5/PDE6 catalytic domain and gain-of-function mutagenesis of the PDE5 catalytic domain. This analysis revealed the key role of PDE6-specific residues within the catalytic domain M-loop−α-helix 15 region and suggested an important contribution of the H-loop−M-loop interface to the PDE6 inhibition by the Pγ C-terminus. Identification of the determinants for the PDE6−Pγ interaction offers insights into the evolution of the visual effector enzyme.

Photoreceptor cGMP phosphodiesterase (PDE6[1] family) is the effector enzyme in the vertebrate visual transduction cascade. The activity of rod and cone PDE6 catalytic subunits is blocked in the dark by the inhibitory Pγ-subunits (Pγ). The inhibition is relieved upon light stimulation of photoreceptor cells (*1*−*3*). The interaction of PDE6 with Pγ is critical for phototransduction and unique for the PDE6 family of phosphodiesterases (*1*−*4*). It involves at least two binding interfaces; one is between the regulatory GAF domain(s) of PDE6 and the central polycationic Pro-rich region of Pγ, and the second is between the catalytic domain of PDE6 and the C-terminus of Pγ (*5*−*7*). The former interface serves primarily to enhance the affinity of the interaction between PDE6 and Pγ, whereas the latter interface represents the key inhibitory interaction. The C-terminus of Pγ occludes the active site of PDE6, thereby preventing hydrolysis of cGMP (*8*−*10*). Because of the failure of functional expression of PDE6 outside vertebrate photoreceptors, current data on the Pγ contact sites on PDE6 have been developed with the use of chimeric enzymes between PDE6 and PDE5 (*11*−*13*). The catalytic domains of PDE5 (PDE5 cd) and PDE6 (PDE6 cd) display significant sequence homology, specificity for cGMP, and sensitivity to a number of common catalytic site inhibitors but are different in that PDE5 cd is not inhibited by Pγ (*11*, *14*). However, a replacement of just one segment corresponding to the M-loop−α-helix 15 region in PDE5 cd with the corresponding sequence of cone PDE6C yields a chimeric catalytic domain, PDE5/6 cd, capable of potent inhibition by Pγ or the Pγ C-terminal peptides (Figure 1A) (*10*, *15*). The crystal structure of the complex between the IBMX-bound PDE5/6 cd and the Pγ C-terminal peptide $Pγ_{70–87}$ has recently been determined (*10*). This structure provided the first detailed picture of the binding site and suggested the determinants for the interaction with Pγ. The $Pγ_{70–87}$ binding surface of PDE5/6 cd is comprised of four structural elements, α-helices 12 and 15 and two variable H- and M-loops (Figure 1B) (*10*). The Pγ-binding segment in helix 12 is conserved between PDE5 and PDE6 and assumes similar conformations in the structures of PDE5 cd and PDE5/6 cd. Therefore, helix 12 does not appear to contribute to the specificity of the Pγ-binding site. Although helix 15 is conformationally similar in the structures of PDE5 cd and PDE5/6 cd, it is important to the specificity of the Pγ−PDE6 interaction in providing essential PDE6-specific Pγ contact residue Phe^{823}. The H- and M-loop conformations are markedly different in the PDE5/6 cd and PDE5 cd structures (*10*, *16*). In PDE5/6 cd, these loops are stabilized by extensive interloop interactions not seen in PDE5 cd (*10*, *16*). Since the H-loop sequence is identical in PDE5/6 cd and PDE5 cd, the ability to establish the interloop interface is dictated by the M-loop. Thus, the M-loop in PDE6 can contribute to the C-terminus of Pγ binding directly by donating specific Pγ contact residues or indirectly by inducing the H-loop−M-loop interface to favorably position residues from both loops for the interaction with Pγ. Here, we performed mutational analysis of the Pγ contact residues and the H-loop−M-loop interface. Using inhibition of PDE activity by the Pγ C-terminal peptide, $Pγ_{63–87}$, as functional readout, loss-of-function and gain-of-function mutations were introduced into PDE5/6 cd and PDE5 cd, respectively. This analysis defined multiple structural determinants of PDE6 inhibition by the C-terminus of Pγ.

EXPERIMENTAL PROCEDURES

Materials. [^{3}H]cGMP was purchased from Amersham Pharmacia Biotech. All restriction enzymes were purchased from NEB. Pfu turbo DNA polymerase was a product of Stratagene. Mini protease inhibitor cocktail tablets were from Roche Molecular Biochemicals. The DNA miniprep kit was purchased from Qiagen. His-bind resin was obtained from Novagen. AG1-X2 cation exchange resin was a product of Bio-Rad. All other reagents were purchased from Sigma. The synthetic peptide corresponding to $Pγ_{63–87}$ was custom-made by Sigma-Genosys and purified by reverse-phase HPLC.

Mutagenesis and Isolation of Mutant PDE5/6 cd and PDE5 cd. The DNA sequence corresponding to human PDE5 residues 535−860 was amplified by RT-PCR with primers

†This work was supported by National Institutes of Health Grant EY-10843.

*To whom correspondence should be addressed. Telephone: (319) 335-7864. Fax: (319) 335-7330. E-mail: nikolai-artemyev@uiowa.edu.

[1]Abbreviations: PDE, cGMP phosphodiesterase; PDE6, photoreceptor PDE; Pγ, γ-subunit of PDE6; PDE5, cGMP-binding, cGMP-specific PDE (PDE5 family); PDE5/6 cd, chimeric PDE5/PDE6 catalytic domain; IBMX, 3-isobutyl-1-methylxanthine; PDB, Protein Data Bank.

 Published on Web 04/16/2010

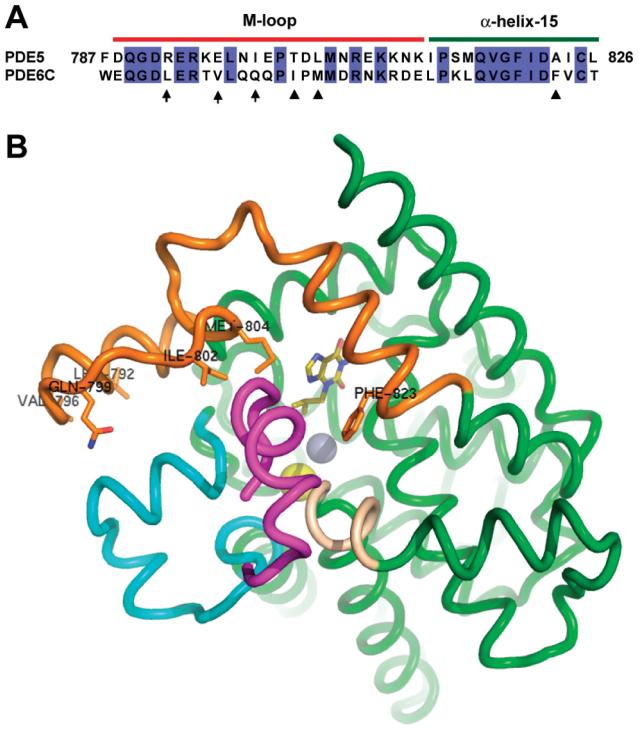

FIGURE 1: (A) Sequence alignment of residues 787−826 of human PDE5 and corresponding residues 746−785 of human cone PDE6C. This region is replaced in PDE5 cd (PDE5 residues 535−860) by PDE6C residues to yield the Pγ-sensitive catalytic domain PDE5/6 cd. The numbering of residues for PDE5/6 cd is the same as for PDE5. Arrows indicate PDE6-specific residues of PDE5/6 cd involved in the H-loop−M-loop interface (Leu^{792}, Val^{796}, and Gln^{799}). Triangles indicate PDE6-specific residues of PDE5/6 cd making direct contacts with the C-terminus of Pγ (Ile^{802}, Met^{804}, and Phe^{823}). (B) Interactions of PDE5/6 cd (green) with Pγ_{70-87} (magenta). Pγ_{70-87} interacts with the M-loop−helix 15 region (orange), the H-loop (cyan), and the N-terminal segment of α-helix 12 (wheat). Leu^{792}, Val^{796}, Gln^{799}, Ile^{802}, Met^{804}, and Phe^{823} are shown as sticks. IBMX is colored olive; the yellow sphere is a magnesium ion and the gray sphere a zinc ion.

containing NdeI and XhoI sites. Total RNA isolated from HEK293 cells was used as a template in the amplification. The PDE5 cd construct was cloned into the pET15b vector (Novagen) using NdeI and XhoI sites. The PDE5/6 cd chimera based on sequences of human PDE5 and PDE6C was generated as described previously (*10*). Mutations were introduced into PDE5/6 cd and PDE5 cd using the QuikChange mutagenesis protocol (Stratagene). Multiple mutations were produced by subsequent mutagenesis of single, double, or triple mutants. The sequences of all constructs were verified by automated DNA sequencing at the University of Iowa DNA Core Facility. The PDE5/6 cd and PDE5 cd mutant plasmids were transformed into BL21-codon plus competent cells (Stratagene). Expression and purification of mutant PDE5/6 cd and PDE5 cd proteins over His-bind resin (Novagen) were performed as previously described (*15*). Isolated recombinant proteins were analyzed by SDS−PAGE in 12% NuPage precast gels (Invitrogen). All PDE5/6 cd and PDE5 cd mutants, except PDE5/6 cd I802A/P803D/M804L/F823A, were expressed as soluble proteins at comparable levels of 4−7 mg/L of culture (Figure 2). The quadrople mutant was expressed at a level of ~2 mg/L.

Characterization of Mutant PDE5/6 cd and PDE5 cd. Mutant PDE5/6 cd and PDE5 cd proteins were analyzed as His$_6$-tagged proteins. Control experiments showed no differences in

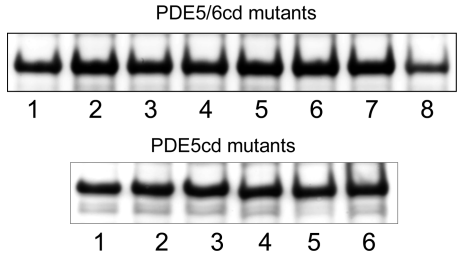

FIGURE 2: Coomassie blue-stained SDS gel with isolated mutant PDE5/6 cd and PDE5 cd proteins. Equal fractions of the preparations from 1 L cultures were loaded as samples. PDE5/6 cd mutants: (1) PDE5/6 cd, (2) I802A, (3) P803D, (4) M804A, (5) A823F, (6) I802A/M804A, (7) L792R/V796E/Q799I, and (8) I802A/P803D/M804L/F823A. PDE5 cd mutants: (1) PDE5 cd, (2) A823F, (3) R792L/E796V/I799Q/A823F, (4) T802I/D803P/L804M/A823F, (5) R792L/E796V/I799Q/T802I/D803P/L804M/A823F, and (6) F787W/R792L/E796V/I799Q/T802I/D803P/L804M/A823F.

the stability, catalytic properties, or Pγ_{63-87} inhibition of these mutants prior to or after removal of the His$_6$ tag with thrombin. PDE activity was measured using 1 μM [^{3}H]cGMP and 5 nM mutant PDE5/6 cd or PDE5 cd according to published protocols (*15*). The K_M and k_{cat} values for cGMP hydrolysis and the K_i for inhibition by Pγ_{63-87} were determined as described previously (*15*). The K_M, k_{cat}, and K_i values are expressed as means ± the standard error for three separate experiments.

RESULTS

Mutational Analysis of the PDE6-Specific Pγ Contact Residues within the M-Loop−α-Helix 15 Region. Replacement of the M-loop−helix 15 region of PDE5 cd with the corresponding region of PDE6 allows for a potent inhibition of the chimeric catalytic domain PDE5/6 cd by the Pγ C-terminal peptides (Figure 1) (*10*, *15*). Accordingly, Pγ_{63-87} had no appreciable effect on the activity of PDE5 cd when tested at concentrations up to 600 μM, and it inhibited PDE5/6 cd with a K_i of 1.7 ± 0.2 μM (Figure 3A and Table 1). The K_M and k_{cat} values of PDE5 cd (3.3 ± 0.4 μM and 0.8 ± 0.2 s^{-1}, respectively) and PDE5/6 cd (3.1 ± 0.5 μM and 0.6 ± 0.1 s^{-1}, respectively) for cGMP hydrolysis were comparable. The crystal structure of PDE5/6 cd in complex with IBMX and Pγ_{70-87} reveals three major PDE6-specific Pγ contact residues within this region, Ile^{802}, Met^{804}, and Phe^{823} (Figure 1) (*10*). These residues are absolutely conserved in the PDE6 family and correspond to a nonconserved residue at position 802 (Ala, Thr, or Ile) and conserved Leu^{804} and Ala^{823} in the PDE5 family (Figure 1A and Figure S1 of the Supporting Information). The role for Met and Phe residues in the PDE6−Pγ interaction was previously recognized, whereas the significance of the Ile residue was unnoticed (*12*, *13*). Indeed, the M804A and F823A mutations resulted in ~6- and ~9-fold reductions in the potency of PDE5/6 cd inhibition by Pγ_{63-87}, respectively (Figure 3A and Table 1). The M804L substitution is a conservative one. This mutation, unlike M804A, had no significant effect on the interaction of PDE5/6 cd with the Pγ peptide (Table 1). Two mutations, I802A and I802T, were introduced into PDE5/6 cd to examine the contribution of Ile^{802}. The I802A and I802T substitutions comparably increased the K_i values for the peptide inhibition of PDE5/6 cd by ~7- and ~5-fold, respectively (Figure 3A and Table 1). Replacement of both M-loop Pγ contacts Ile^{802} and Met^{804} with Ala residues cumulatively impaired the interaction of PDE5/6 cd with Pγ_{63-87}. The double PDE5/6 cd mutant

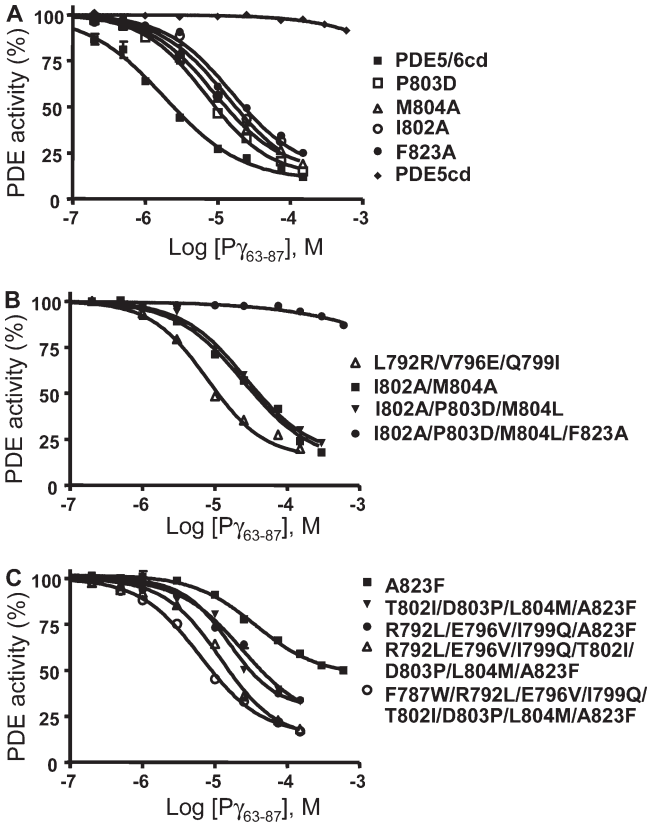

FIGURE 3: Inhibition of mutant PDE5/6 cd and PDE5 cd by $P\gamma_{63-87}$. The activities of PDE5/6 cd and PDE5 cd (A) or PDE5/6 cd mutants (A and B) and PDE5 cd mutants (C) were measured in the presence of 1 μM cGMP and increasing concentrations of $P\gamma_{63-87}$. PDE activity is expressed as a percentage of that in the absence of $P\gamma_{63-87}$. Results of representative experiments are shown. The K_i values are listed in Table 1 as means ± the standard error from three similar experiments.

I802A/M804A was inhibited by the peptide with a K_i of 26.2 ± 3.0 μM (Figure 3B and Table 1).

Ile[802] and Met[804] in PDE5/6 cd are separated by a conserved PDE6-specific Pro[803] (Figure S1 of the Supporting Information). Pro[803] was substituted with a conserved PDE5 residue Asp[803] to test Pro[803]'s potential influence on the conformation of the Pγ contacts and the architecture of the M-loop. The P803D mutation led to an ~4-fold decrease in the affinity of PDE5/6 cd for $P\gamma_{63-87}$ (Figure 3A). The effect of combined replacement of the M-loop segment Ile[802]Pro[803]Met[804] with the PDE5-specific residues Ala[802]Asp[803]Leu[804] (bovine PDE5) or Thr[802]Asp[803]Leu[804] (human PDE5) was an ~15- or ~13-fold reduction in the efficiency of PDE5/6 cd inhibition by $P\gamma_{63-87}$, respectively (Figure 3B and Table 1). All three PDE6-specific Pγ contact residues were swapped with PDE5 residues in a PDE5/6 cd quadruple mutant (I802A/P803D/M804L/F823A). This mutant was expressed at a lower level compared to the other PDE5/6 cd mutants (Figure 2). However, the mutant folding was not significantly impaired, since its K_M (4.0 ± 0.3 μM) and k_{cat} (0.5 s^{-1}) values were similar to those of PDE5/6 cd. The PDE5/6 cd quadruple mutant was not appreciably inhibited by $P\gamma_{63-87}$ (Figure 3B and Table 1).

Mutational Analysis of the H-Loop−M-Loop Interface. Conformations of the H- and M-loops in the PDE5/6 cd−IBMX−$P\gamma_{70-87}$ and PDE5 cd−IBMX structures are distinctly different (*10*, *16*). The H- and M-loops in PDE5/6 cd are stabilized by an extensive interloop interface. Residues Val[660] and Tyr[664] of the H-loop make hydrophobic interactions with

Table 1: Inhibition of Mutant PDE5/6 cd and PDE5 cd by $P\gamma_{63-87}$

	K_M (μM)	K_i for $P\gamma_{63-87}$ (μM)
PDE5/6 cd and Mutants		
PDE5/6 cd[a]	3.1 ± 0.5	1.7 ± 0.2
L792R	3.4 ± 0.6	3.2 ± 0.3
V796E	4.1 ± 0.2	1.8 ± 0.1
Q799I	3.2 ± 0.8	3.5 ± 0.3
L792R/V796E/Q799I	3.5 ± 0.9	6.0 ± 0.6
I802A	2.9 ± 0.2	12.1 ± 2.1
I802T	3.9 ± 0.6	8.6 ± 0.3
P803D	3.0 ± 0.2	6.7 ± 0.5
M804A	2.8 ± 0.7	10.3 ± 1.6
M804L	2.9 ± 0.6	2.0 ± 0.1
F823A	3.0 ± 0.7	15.1 ± 1.7
I802A/M804A	3.2 ± 0.7	26.2 ± 3.0
I802A/P803D/M804L	3.8 ± 0.1	25.5 ± 2.6
I802T/P803D/M804L	2.5 ± 0.2	21.8 ± 1.8
I802A/P803D/M804L/F823A	4.0 ± 0.3	> 3000
PDE5 cd and Mutants		
PDE5 cd[a]	3.3 ± 0.4	> 10000
A823F	3.7 ± 0.3	44.3 ± 4.5 (52 ± 4)[b]
A823F with $P\gamma_{63-87}$ (150 μM)	4.0 ± 0.4	
R792L/E796V/I799Q/A823F	4.0 ± 0.4	23.5 ± 3.4 (78 ± 5)[b]
T802I/D803P/L804M/A823F	2.8 ± 0.6	19.4 ± 0.1 (72 ± 4)[b]
R792L/E796V/I799Q/T802I/ D803P/L804M/A823F	3.2 ± 0.7	10.2 ± 0.7
F787W/R792L/E796V/I799Q/ T802I/D803P/L804M/A823F	3.7 ± 0.4	5.8 ± 0.4

[a]The k_{cat} values for PDE5/6 cd and PDE5 cd were 0.6 ± 0.1 and 0.8 ± 0.2 s^{-1}, respectively. The k_{cat} values of the mutants were comparable to the parent protein k_{cat}. [b]Values in parentheses indicate maximal inhibition (percent). Maximal inhibition values for other mutants are greater than 85%.

M-loop residues Leu[792], Val[796], and Leu[797], whereas polar residues Asn[661] and Arg[667] in the H-loop form contacts with residues Gln[789], Glu[793], and Gln[799] in the M-loop (*10*). Three of the M-loop residues involved in the interface with the H-loop, Leu[792], Val[796], and Gln[799], are strongly conserved in PDE6 and differ from the corresponding residues in PDE5, Arg(Lys)[792], Glu[796], and Ile(Met)[799] (Figure S1 of the Supporting Information). To probe the role of the H-loop−M-loop interface in stabilizing the Pγ-binding surface, Leu[792], Val[796], and Gln[799] of PDE5/6 cd were mutated singly or in combination to PDE5-specific residues. The L792R and Q799I substitutions each resulted in a modest ~2-fold attenuation of the PDE5/6 cd affinity for $P\gamma_{63-87}$, while the V796E mutation had no effect (Table 1). Consistent with the effects of the single mutations, the triple mutant L792R/V796E/Q799I displayed a moderate 3.5-fold impairment of the affinity of the interaction with the Pγ peptide (Figure 3B).

Gain-of-Function Mutations of the M-Loop−α-Helix 15 Region in PDE5/6 cd. To further examine the role of the M-loop and its interface with the H-loop for the PDE6−Pγ interaction in a gain-of-function approach, we first restored the critical α-helix 15 Pγ contact residue by replacing Ala[823] of PDE5 cd with Phe. The A823F mutant of PDE5 cd acquired sensitivity to $P\gamma_{63-87}$ with a K_i of 44.3 ± 4.5 μM, although the maximal inhibition was only partial (~52%) (Figure 3C and Table 1). The K_M value of the mutant was unchanged in the presence of $P\gamma_{63-87}$, suggesting that the inhibition by the peptide was allosteric (Table 1). The PDE5 cd A823F mutant was then used as a template to introduce PDE6-specific M-loop residues

essential for direct interactions with the H-loop (Leu^{792}, Val^{796}, and Gln^{799}) or Pγ (Ile^{802}, Pro^{803}, and Met^{804}). Both PDE5 cd quadruple mutants, R792L/E796V/I799Q/A823F and T802I/D803P/L804M/A823F, exhibited improved maximal inhibition and an ~2−3-fold enhancement of the affinity of interaction with Pγ_{63-87} in comparison to that of the A823F mutant (Figure 3C and Table 1). The effect of the former quadruple mutation matched the loss of affinity for Pγ_{63-87} in the reciprocal L792R/V796E/Q799I mutant of PDE5/6 cd. However, the effect of the latter quadruple mutation was smaller than the ~13-fold increase in the K_i value for the reverse I802T/P803D/M804L mutant of PDE5/6 cd, suggesting that residues Ile^{802}, Pro^{803}, and Met^{804} are not as well conformationally positioned for the interaction with Pγ_{63-87} in the context of the PDE5 cd mutant as they are in PDE5/6 cd. Incorporation of the two clusters of mutations, R792L/E796V/I799Q and T802I/D803P/L804M, into the A823F mutant background had a cumulative effect (Figure 3C). The resulting PDE5 cd mutant was inhibited by Pγ_{63-87} with a K_i of 10.2 ± 0.7 μM (Figure 3C and Table 1). Still, this PDE5 cd mutant was less sensitive to Pγ than PDE5/6 cd, indicating additional structural determinants for binding the C-terminus of Pγ. In the PDE5/6 cd structure, conserved PDE6-specific residue Trp^{787} buttresses the M-loop backbone at residues Asp^{805}, Arg^{806}, and Asn^{807}, thereby possibly affecting or stabilizing conformations of Ile^{802} and Met^{804} (*10*). Phe^{787}, a PDE5 counterpart of Trp^{787} is less bulky and might provide less support for the M-loop. Indeed, the additional F787W mutation increased the potency of the inhibition by Pγ_{63-87} (Figure 3C and Table 1).

DISCUSSION

The unique ability of PDE6 enzymes to interact with the Pγ subunits is critical for vertebrate vision and may have evolved along with the evolution of the PDE6 family and the vertebrate phototransduction cascade (*1*−*3*, *17*). The phylogenetic analysis of PDEs and the gene structure similarities indicate the common ancestry of PDE6 with PDE5 and PDE11 (*17*, *18*). PDE5 is also similar to PDE6 in biochemical characteristics such as substrate specificity and sensitivity to common catalytic site inhibitors (*14*, *19*). The common ancestry and biochemical similarities make PDE5 cd perhaps the most useful template among all PDE families for studying the determinants of the inhibitory interaction of PDE6 cd with the C-terminus of Pγ. Chimeric PDE5/6 cd containing a relatively short 40-amino acid residue segment of PDE6 encompassing the M-loop and helix 15 was shown to be inhibited in a manner comparable to that of native PDE6 by the Pγ_{63-87} peptide (Figure 1A) (*10*, *15*). Thus, the inhibition determinants are almost entirely confined to this segment of PDE6. The crystal structure of Pγ_{70-83} bound to PDE5/6 cd reveals two Pγ contact residues within the M-loop (Ile^{802} and Met^{804}) and one Pγ contact residue within helix 15 (Phe^{823}) that differ from the corresponding residues of PDE5 cd (Figure 1B) (*10*). Consistent with the structure of the PDE5/6 cd−Pγ_{70-87} complex, replacement of any of these residues with Ala significantly reduces the potency of PDE5/6 cd inhibition by Pγ_{63-87}. Nevertheless, PDE5-specific Leu^{804} is fully capable of substituting Met^{804} in the interaction with Pγ_{63-87} which is evident from the analysis of the PDE5/6 cd M804L mutant. Also, PDE5 in some lower vertebrate species contains an Ile at position 802 (Figure S1 of the Supporting Information). An additional factor contributing to the M-loop−Pγ interaction is the PDE6-specific Pro^{803} that appears to be important in the positioning of Ile^{802} and Met^{804} (Figure 3A). It is unlikely that the effect of the P803D substitution in PDE5/6 cd is due to repulsive interactions of the Asp residue with the negatively charged Pγ peptide. On the basis of the complex structure, the distance between Pro^{803} and the closest acidic residue of Pγ, Glu^{80}, exceeds 10 Å (*10*). The PDE5/6 cd mutant I802A/P803D/M804L/F823A with all three Pγ-interacting residues and Pro^{803} substituted by PDE5 counterparts was insensitive to Pγ_{63-87} (Figure 3B). Thus, the lack of inhibition of PDE5 cd by the Pγ C-terminal peptide can be largely attributed to the disruption of these contacts.

Comparison of the structures of PDE5/6 cd and PDE5 cd also suggests that conformational differences between the catalytic domains may constitute a major determinant for the interaction with the C-terminus of Pγ. The structures of PDE5/6 cd and PDE5 cd are closely superimposable except for the H- and M-loops, both of which participate in the interaction with Pγ_{70-87} (*10*, *16*). An extensive interloop interface in PDE5/6 cd stabilizes the H- and M-loop in the conformations that favor Pγ binding. In structures of several PDE catalytic domains with bound IBMX, the H-loop and the M-loop interact with each other and adopt conformations reminiscent of the PDE5/6 cd fold (*20*−*22*). In contrast, in the PDE5 cd structure, the M-loop points away from the H-loop, the catalytic cavity, and the projected Pγ_{70-87} binding surface, and residues 793−807 are disordered (*16*). Surprisingly, the disruption of the H-loop−M-loop interface in the PDE5/6 cd L792R/V796E/Q799I mutant resulted in an only modest 3.5-fold decrease in the PDE5/6 cd affinity for Pγ_{63-87}. If the H- and M-loops of PDE5/6 cd would assume the PDE5-like conformations, a much greater impairment of the interaction is predicted. We hypothesize that the lack of a stronger effect of the L792R/V796E/Q799I mutation is due to the ability of Pγ_{63-87} to induce conformations of the H- and M-loops that are similar to the interloop interface-supported conformations. The interloop interface and induced fit binding of Pγ_{63-87} may cooperatively contribute to the interaction of the C-terminus of Pγ with the catalytic domain of PDE6C. The results of gain-of-function experiments are in agreement with this hypothesis. The maximal inhibition of the PDE5 cd A823F mutant by Pγ_{63-87} is only partial (Figure 3C), implying that cGMP can access the active site when the Pγ peptide is bound to the catalytic domain. In the superimposed model of the PDE5 cd−IBMX structure and the PDE5/6 cd−IBMX−Pγ_{70-87} structure, there is a large opening between the H- and M-loops of PDE5 cd and Pγ_{70-87} that allows diffusion of cGMP into the catalytic cavity (Figure 4). Bound Pγ_{63-87} does not affect the affinity (K_M) of PDE5 cd A823F for cGMP (Table 1). The noncompetitive mechanism of PDE5 cd A823F inhibition by Pγ_{63-87} is in accord with the notion that Pγ is a noncompetitive inhibitor of PDE6. In the PDE5/6 cd−IBMX−Pγ_{70-87} structure, the C-terminus of Pγ does not interact or clash with IBMX (*10*). Similarly, in the superimposed model of the PDE5/6 cd−IBMX−Pγ_{70-87} structure and the structure of the PDE10A2 D674A mutant in complex with cGMP (*23*), there are no contacts or clashes between Pγ_{70-87} and cGMP (Figure S2 of the Supporting Information). Furthermore, a recent study directly demonstrated that the inhibiton of PDE6 by Pγ_{63-87} is noncompetitive when cGMP is used as a substrate (*24*). The allosteric inhibitory effect of Pγ_{63-87} on PDE5 cd A823F may have resulted from conformational changes in the metal binding subpocket of the active site induced by the interaction of the peptide with α-helix 12 and/or the H-loop. Interestingly, an allosteric component to the Pγ

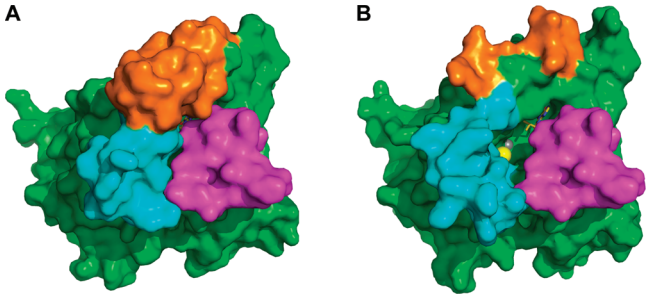

FIGURE 4: (A) Surface representation of PDE5/6 cd (green) with IBMX and Pγ_{70-87} bound (magenta). The H-loop is colored cyan and the M-loop orange. Pγ_{70-87} entirely occludes the opening of the catalytic pocket. (B) The IBMX-bound PDE5 cd (PDB entry 1RKP) was structurally aligned with PDE5/6 cd (PDB entry 3JWR, chain A) bound with Pγ_{70-87} (PDB entry 3JWR, chain C) using PyMOL version 1.2r2 (*26*). The PDE5/6 cd structure is omitted from the superimposed model, and the PDE5 cd structure and Pγ_{70-87} are shown in surface representation. In the model, an opening exists between the H- and M-loops of PDE5 cd and Pγ_{70-87} that allows access to the catalytic pocket. IBMX is colored olive; the yellow sphere is a magnesium ion and the gray sphere a zinc ion.

inhibition of PDE6 has been recently recognized (*24*). Using the PDE5 cd A823F template, we have shown that mutations promoting formation of the interloop interface or introducing the PDE6-specific Pγ-binding Ile^{802}Pro^{803}Met^{804} motif into the M-loop increased the affinity of the catalytic domain for Pγ_{63-87} and augmented the maximal inhibition effect (Figure 3C). Thus, the interaction of Pγ with the M-loop apparently induces a conformational change in PDE5 cd mutants similar to that of the interloop interface, i.e., a shift of the M-loop toward the catalytic cavity and the H-loop. Mutant PDE5 cd catalytic domains containing the Pγ contact residues from the M-loop−helix 15 region and the interloop interface residues are inhibited by Pγ_{63-87} fully, but not as potently as PDE5/6 cd. An additional Pγ interaction determinant was identified. A conserved PDE6-specific residue Trp^{787} is likely to support the M-loop conformation favorable for the binding of Pγ_{63-87}. Among 22 residue positions that are different in PDE5/6 cd and PDE5 cd (Figure 1A), eight positions were examined by mutagenesis in this study. The collective contribution of the 14 remaining PDE6-specific residues of PDE5/6 cd to the interaction with Pγ is small, and the PDE5/6 cd−Pγ_{70-87} structure does not indicate particular contributing residues. A number of the 14 uncharacterized residues may exert a minor influence on the conformation of the M-loop−helix 15 region. In addition, the PDE5/6 cd−Pγ_{70-87} structure apparently recaptures most, but not all, contacts between PDE6 and the C-terminus of Pγ, because Pγ_{70-87} inhibits PDE5/6 cd somewhat less potently than Pγ_{63-87} (*10*). Thus, additional unidentified PDE6 determinants for the interaction with the C-terminus of Pγ are possible.

When did the capacity of PDE6 enzymes for inhibition by Pγ evolve? PDE6 from the lamprey *Petromyzon marinus*, representing the earliest surviving vertebrate class of jawless fish, is highly conserved with PDE6 from higher vertebrates (*17*). The catalytic domain of lamprey PDE6 is ~80% identical to the catalytic domains of human cone and rod PDE6 enzymes, and it contains all of the structural determinants for the interaction with the C-terminus of Pγ identified in this study. The Pγ subunits in *P. marinus* inhibit lamprey's PDE6 in a manner equivalent to that for the PDE6 inhibition in higher vertebrates (*17*). A PDE6−related enzyme has been identified in tunicates *Ciona savignyi* and *Ciona intestinalis*. Ciona's PDE6 is highly divergent from vertebrate PDE6s, but it groups together with the PDE6 family by phylogenetic analysis (*17*). Tunicates (urochordates) are the closest living relatives of vertebrates (*25*). The evolution of the PDE6 family appears to have begun prior to the last common ancestor of tunicates and vertebrates. Current genome databases provide no indication of the presence of Pγ genes in invertebrate species. Nonetheless, reconstruction of ancestral PDE6 and PDE5/6/11 enzymes suggests that they contained the M-loop Pγ-binding signature motif Ile-Pro-Met, and they may have been predisposed to the interaction with Pγ (Figure S3 of the Supporting Information). Intriguingly, prebilaterian cnidarians *Nematostella vectensis* and *Hydra magnipapillata* have PDE5/6-like enzymes that contain an essential Phe in α-helix 15 in addition to the Ile-Pro-Met motif (Figure S3 of the Supporting Information). Our analysis predicts that these enzymes are capable of effective interaction with the C-terminus of Pγ. Thus, the PDE capacity for binding Pγ predated the emergence of the inhibitory subunit, an ultimate step in the evolution of the visual effector.

ACKNOWLEDGMENT

We thank Dr. H. Muradov for cloning of the catalytic domain of human PDE5.

SUPPORTING INFORMATION AVAILABLE

Multiple-sequence alignments of the M-loop−α-helix 15 regions of PDE6 and PDE5 from various species (Figure S1), superimposed model of the PDE5/6 cd−IBMX−Pγ_{70-87} structure and the structure of the PDE10A2 D674A mutant in complex with cGMP (Figure S2), and sequence alignment of the M-loop−α-helix 15 regions of the reconstructed ancestral PDE6 and PDE5/6/11 enzymes, as well as the PDE5/6-like enzymes from *Nematostella vectensis* and *Hydra magnipapillata* (Figure S3). This material is available free of charge via the Internet at http://pubs.acs.org.

REFERENCES

1. Arshavsky, V. Y., Lamb, T. D., and Pugh, E. N., Jr. (2002) G proteins and phototransduction. *Annu. Rev. Physiol. 64*, 153–187.
2. Lamb, T. D., and Pugh, E. N., Jr. (2006) Phototransduction, dark adaptation, and rhodopsin regeneration the proctor lecture. *Invest. Ophthalmol. Visual Sci. 47*, 5137–5152.
3. Fu, Y., and Yau, K. W. (2007) Phototransduction in mouse rods and cones. *Pfluegers Arch. 454*, 805–819.
4. Conti, M., and Beavo, J. (2007) Biochemistry and physiology of cyclic nucleotide phosphodiesterases: Essential components in cyclic nucleotide signaling. *Annu. Rev. Biochem. 76*, 481–511.
5. Artemyev, N. O., and Hamm, H. E. (1992) Two-site high-affinity interaction between inhibitory and catalytic subunits of rod cyclic GMP phosphodiesterase. *Biochem. J. 283*, 273–279.
6. Mou, H., and Cote, R. H. (2001) The catalytic and GAF domains of the rod cGMP phosphodiesterase (PDE6) heterodimer are regulated by distinct regions of its inhibitory γ subunit. *J. Biol. Chem. 276*, 27527–27534.
7. Guo, L. W., Muradov, H., Hajipour, A. R., Sievert, M. K., Artemyev, N. O., and Ruoho, A. E. (2006) The inhibitory γ subunit of the rod cGMP phosphodiesterase binds the catalytic subunits in an extended linear structure. *J. Biol. Chem. 281*, 15412–15422.
8. Artemyev, N. O., Natochin, M., Busman, M., Schey, K. L., and Hamm, H. E. (1996) Mechanism of photoreceptor PDE inhibition by its γ-subunits. *Proc. Natl. Acad. Sci. U.S.A. 93*, 5407–5412.
9. Granovsky, A. E., Natochin, M., and Artemyev, N. O. (1997) The γ-subunit of rod cGMP-phosphodiesterase blocks the enzyme catalytic site. *J. Biol. Chem. 272*, 11686–11669.
10. Barren, B., Gakhar, L., Muradov, H., Boyd, K., Ramaswamy, S., and Artemyev, N. O. (2009) Structural basis of phosphodiesterase 6 inhibition by the γ-subunit. *EMBO J. 28*, 3613–3622.

11. Granovsky, A. E., Natochin, M., McEntaffer, R. L., Haik, T. L., Francis, S. H., Corbin, J. D., and Artemyev, N. O. (1998) Probing domain functions of chimeric PDE6α′/PDE5 cGMP-phosphodiesterase. *J. Biol. Chem. 273*, 24485–24490.
12. Granovsky, A. E., and Artemyev, N. O. (2000) Identification of the γ-subunit interacting residues on photoreceptor cGMP phosphodiesterase, PDE6α′. *J. Biol. Chem. 275*, 41258–41262.
13. Granovsky, A. E., and Artemyev, N. O. (2001) Partial reconstitution of photoreceptor cGMP phosphodiesterase characteristics in cGMP phosphodiesterase-5. *J. Biol. Chem. 276*, 21698–21703.
14. Cote, R. H. (2004) Characteristics of photoreceptor PDE (PDE6): Similarities and differences to PDE5. *Int. J. Impotence Res. 16* (Suppl. 1), S28–S33.
15. Muradov, K. G., Boyd, K. K., and Artemyev, N. O. (2006) Analysis of PDE6 function using chimeric PDE5/6 catalytic domains. *Vision Res. 46*, 860–868.
16. Huai, Q., Liu, Y., Francis, S. H., Corbin, J. D., and Ke, H. (2004) Crystal structures of phosphodiesterases 4 and 5 in complex with inhibitor 3-isobutyl-1-methylxanthine suggest a conformation determinant of inhibitor selectivity. *J. Biol. Chem. 279*, 13095–13101.
17. Muradov, K. G., Boyd, K. K., Kerov, V., and Artemyev, N. O. (2007) PDE6 in lamprey *Petromyzon marinus*: Implications for the evolution of the visual effector in vertebrates. *Biochemistry 46*, 9992–10000.
18. Yuasa, K., Kanoh, Y., Okumura, K., and Omori, K. (2001) Genomic organization of the human phosphodiesterase PDE11A gene. Evolutionary relatedness with other PDEs containing GAF domains. *Eur. J. Biochem. 268*, 168–178.
19. Francis, S. H., Corbin, J. D., and Bischoff, E. (2009) Cyclic GMP-hydrolyzing phosphodiesterases. *Handb. Exp. Pharmacol. 191*, 367–408.
20. Scapin, G., Patel, S. B., Chung, C., Varnerin, J. P., Edmondson, S. D., Mastracchio, A., Parmee, E. R., Singh, S. B., Becker, J. W., Van der Ploeg, L. H., and Tota, M. R. (2004) Crystal structure of human phosphodiesterase 3B: Atomic basis for substrate and inhibitor specificity. *Biochemistry 43*, 6091–6100.
21. Huai, Q., Wang, H., Zhang, W., Colman, R. W., Robinson, H., and Ke, H. (2004) Crystal structure of phosphodiesterase 9 shows orientation variation of inhibitor 3-isobutyl-1-methylxanthine binding. *Proc. Natl. Acad. Sci. U.S.A. 101*, 9624–9629.
22. Pandit, J., Forman, M. D., Fennell, K. F., Dillman, K. S., and Menniti, F. S. (2009) Mechanism for the allosteric regulation of phosphodiesterase 2A deduced from the X-ray structure of a near full-length construct. *Proc. Natl. Acad. Sci. U.S.A. 106*, 18225–182030.
23. Wang, H., Liu, Y., Hou, J., Zheng, M., Robinson, H., and Ke, H. (2007) Structural insight into substrate specificity of phosphodiesterase 10. *Proc. Natl. Acad. Sci. U.S.A. 104*, 5782–5787.
24. Zhang, X. J., Skiba, N. P., and Cote, R. H. (2010) Structural requirements of the photoreceptor phosphodiesterase γ-subunit for inhibition of rod PDE6 holoenzyme and for its activation by transducin. *J. Biol. Chem. 285*, 4455–4463.
25. Delsuc, F., Brinkmann, H., Chourrout, D., and Philippe, H. (2006) Tunicates and not cephalochordates are the closest living relatives of vertebrates. *Nature 439*, 965–968.
26. DeLano, W. L. (2004) The PyMOL molecular graphics system, DeLano Scientific, San Carlos, CA.